Parity non-conservation in the alpha particle decay of the 8.87 MeV 2^- state of ^{16}O

K. Neubeck,* H. Schober, and H. Wäffler
Nuclear Physics Division, Max-Planck-Institute for Chemistry, 6500 Mainz, Germany

(Received 22 August 1973; revised manuscript received 27 March 1974)

The energy spectrum of 2.5×10^8 α particles from the sequential decay $^{16}N(\beta^-)^{16}O(\alpha)^{12}C$ has been analyzed. Superimposed on the broad energy distribution which originated from the decay of the 1^- 9.60 MeV state of ^{16}O into $^{12}C+\alpha$, a group of 9538 ± 1810 α particles with an energy of 1282 keV has been identified with a maximum error of ±5 keV. This group is attributed to the parity non-conserving decay from the 2^- 8.87 MeV state of ^{16}O into $^{12}C+\alpha$; the α-particle emission width for this decay has been determined to be $\Gamma_\alpha = (1.03\pm0.28)\times10^{-10}$ eV. In a separate measurement the relative ^{16}N β decay branching ratio to the 9.60 and 8.87 MeV states in ^{16}O, which was necessary for the calculation of Γ_α, has been determined to be $(9.98\pm0.70)\times10^{-4}$.

[RADIOACTIVITY $^{16}N(\beta^-)^{16}O(\alpha)^{12}C$; measured energy spectrum; deduced α-particle group $E_\alpha = 1282\pm5$ keV attributed to parity non-conserving α-particle decay $^{16}O(8.87\ \text{MeV}\ 2^-)\rightarrow{}^{12}C+\alpha$; deduced $\Gamma_\alpha = (1.03\pm0.28)\times10^{-10}$ eV.]

1. INTRODUCTION

Parity non-conservation in hadronic interactions has the consequence that the wave function ψ of a nuclear state will no longer have a definite parity. However, if the parity non-conserving part of the nuclear force is small the wave function will consist of a dominant part with the nominal parity (π) and a small admixture of wave functions of neighbouring states ψ_n with opposite parity $(-\pi)$:

$$\psi = \psi_0^{(\pi)} + \sum_n F_n \psi_n^{(-\pi)}. \tag{1.1}$$

In the context of first order perturbation theory, the amplitudes F_n are given by the expression

$$F_n = \frac{\langle \psi_n^{(-\pi)} | V^{\text{pnc}} | \psi_0^{(\pi)} \rangle}{E_0 - E_n}, \tag{1.2}$$

where V^{pnc} is the parity non-conserving nuclear force potential, E_0 is the energy of the state $|\psi_0^{(\pi)}\rangle$, and E_n is the energy of the state $\langle\psi_n^{(-\pi)}|$.

In 1958 Wilkinson[1] proposed three types of experiments in which parity non-conservation might be observed: (i) circular polarization of nuclear γ rays, (ii) left-right asymmetry in γ-ray emission after capture of polarized nucleons, and (iii) α-particle emission from unnatural parity states in self-conjugate nuclei. The first two types of experiments are indirect in that they use electromagnetic transitions to determine parity mixing in the nuclear states involved, but both are interference effects which are directly proportional to the amplitudes F_n of the admixed irregular parity states in Eq. (1.2). The third type of experiment is direct in that only nuclear constituents participate; however, the nuclear level width for α-particle emission is proportional to the square of the nuclear wave function and thus is proportional to F_n^2. The value of F for these processes has been reported[2] as $\approx10^{-6}$, making the expected level width for α-particle emission very small. For this reason successful investigations of parity non-conservation have been to date restricted to only the first two types of experiments (see Ref. 2).

A nuclear state $|\psi\rangle$ of unnatural parity, which is energetically unstable against α decay but stable against disintegration into other fragments, de-excites by radiative transitions if α-particle emission is strictly forbidden by parity conservation. By assuming for simplicity one neighboring state $|\psi_1^{(-\pi)}\rangle$ only to contribute to the parity admixture, the nuclear wave function from Eq. (1.1) becomes

$$\psi = \psi_0^{(\pi)} + F_1 \psi_1^{(-\pi)}. \tag{1.3}$$

The reduced α-particle emission width γ_α is then given by the overlap integral

$$\gamma_\alpha = \langle\alpha|\psi\rangle_a = F_1 \langle\alpha|\psi_1^{(-\pi)}\rangle_a = F_1 \gamma_\alpha^{(-\pi)}, \tag{1.4}$$

where $\langle\alpha|$ is the state vector of the nuclear system dissociated into an α particle and daughter nucleus within the α-decay channel radius a and $\gamma_\alpha^{(-\pi)}$ is the reduced α-particle width of the admixed state. Since $\langle\alpha|$ must have parity $(-\pi)$, only the admixed wave function $\psi_1^{(-\pi)}$ will contribute to the overlap integral in Eq. (1.4). By introducing the Coulomb barrier penetrability $P_\alpha(\epsilon)$, where ϵ is the kinetic energy of the α particle and daughter nucleus in the center of mass system, and using Eq. (1.4), the experimental α-particle emission

width is obtained as

$$\Gamma_\alpha = P_\alpha(\epsilon)\gamma_\alpha^2 = F_1^2\Gamma_\alpha^{(-\pi)}P_\alpha(\epsilon)/P_\alpha(\epsilon_1). \qquad (1.5)$$

In Eq. (1.5), $\Gamma_\alpha^{(-\pi)}$ is the α-particle emission width for the admixed state $|\psi_1^{(-\pi)}\rangle$ and ϵ_1 is the kinetic energy of the α particle and daughter nucleus in that state.

The decay rate of the parity non-conserving α transition which one would like to observe is proportional to the ratio of the level widths Γ_α/Γ where Γ is the total level width for deexcitation of the state $|\psi\rangle$ and can be well approximated by Γ_γ, the total radiation width of this state. A small width Γ_γ is therefore helpful for the detection of parity non-conserving α decay. From this it follows that in even-even nuclei, states with isospin $T=0$ are more favorable for this type of experiment than states with isospin $T=1$, since the lowest order multipole transitions $E1$ and $M1$ between $T=0$ states are inhibited in these nuclei, thus increasing the ratio $\Gamma_\alpha/\Gamma_\gamma$. No hindrance exists for transitions from states with $T=1$ to the lower lying $T=0$ states.

For an experiment in which parity non-conserving α-particle decay is to be investigated, the unnatural parity state of interest must be selectively excited, since the simultaneous excitation of neighboring, natural parity states would create a background from parity-conserving α-particle decay and in this way mask the small parity non-conserving effect. Such a selective excitation can be obtained by using a radioisotope which by allowed β transition leads to the unnatural parity state of interest. The β decay to neighboring states with natural parity is in this case frequently inhibited by selection rules. Furthermore, the recoil of the daughter nucleus produced by the β transition is small, and therefore the width of the energy distribution of the subsequently emitted α particles is in general not greater than the energy resolution of modern surface barrier detectors.

At present the best conditions for an experiment of this type seem to be offered by the 8.87 MeV 2^- ($T=0$) state in ^{16}O which can be populated from the β decay of ^{16}N ($T_{1/2}=7.1$ sec) with a branching ratio of 1.1% (see Fig. 1). This state exceeds the α-particle emission threshold in ^{16}O by 1.71 MeV, has a small width ($\Gamma_\gamma \approx 3\times10^{-3}$ eV), and deexcites to the ground state by γ-ray cascades.

Neglecting the extremely weak β-decay branch from the 9.85 MeV 2^+ state, there is only one other state in ^{16}O above the α-particle emission threshold populated by the β decay of ^{16}N, i.e., the 9.60 MeV 1^- state which deexcites by regular α-particle decay. This state is broad ($\Gamma_\alpha \approx 650$ keV) and therefore its α-particle distribution will overlap with the group of α particles to be expected from

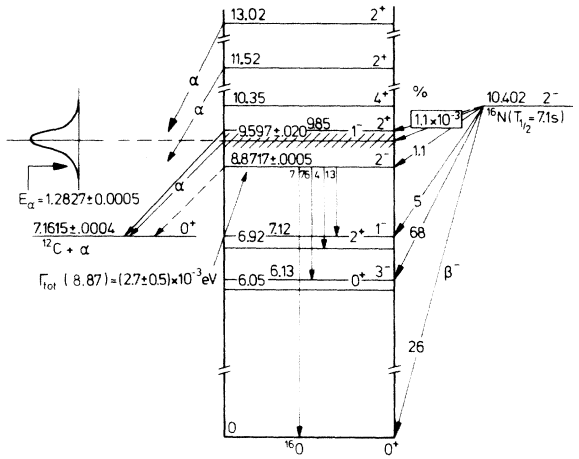

FIG. 1. Level scheme of ^{16}O. The α-particle spectrum from the decay of the 9.60 MeV state is shown on the left. The arrow marks the position of the parity non-conserving α-particle group from the 8.87 MeV 2^- state. Levels not relevant to the experiment are omitted. The energy values (in MeV) are taken from F. Ajzenberg-Selove, Nucl. Phys. A166, 1 (1971).

a parity non-conserving decay of the narrow 8.87 MeV 2^- state. Since the β branching ratio to the 9.60 MeV state is only about 10^{-3}%, the α-particle background from the decay of this state will be relatively small, but still about 100 times greater than the expected peak from the parity non-conserving α-particle decay of the 8.87 MeV state.

During the past decade, several attempts to detect parity non-conservation in the sequential decay of ^{16}N have been reported; the results of these investigations are summarized in Table I. As can be seen from this table, with the exception of Refs. 9 and 10, upper limits only have been obtained for the α-particle emission widths Γ_α of the ^{16}O (8.87 MeV 2^-) state by the different authors. In most of these experiments, it was mainly the lack of sufficiently high α-particle yields which prevented a discrimination of the small group of parity non-

TABLE I. Compilation of published results on the α-particle emission width Γ_α of the ^{16}O(8.87 MeV 2^-) state.

Author	Year	Ref.	Γ_α (eV)
Segel *et al.*	1961	3	$<3.9\times10^{-7}$
Alburger *et al.*	1961	4	$\lesssim 4.8\times10^{-8}$
Kaufmann and Wäffler	1961	5	$<8\times10^{-9}$
Segel *et al.*	1961	6	$<6\times10^{-9}$ ($\Gamma_\alpha/\Gamma_\gamma < 2\times10^{-6}$)
Donovan *et al.*	1961	7	$\lesssim 4.4\times10^{-9}$
Boyd *et al.*	1968	8	$\lesssim 1.1\times10^{-9}$
Sprenkel-Segel *et al.*	1970	9	1×10^{-9}
Hünchen *et al.*	1970	10	$(1.8\pm0.8)\times10^{-10}$

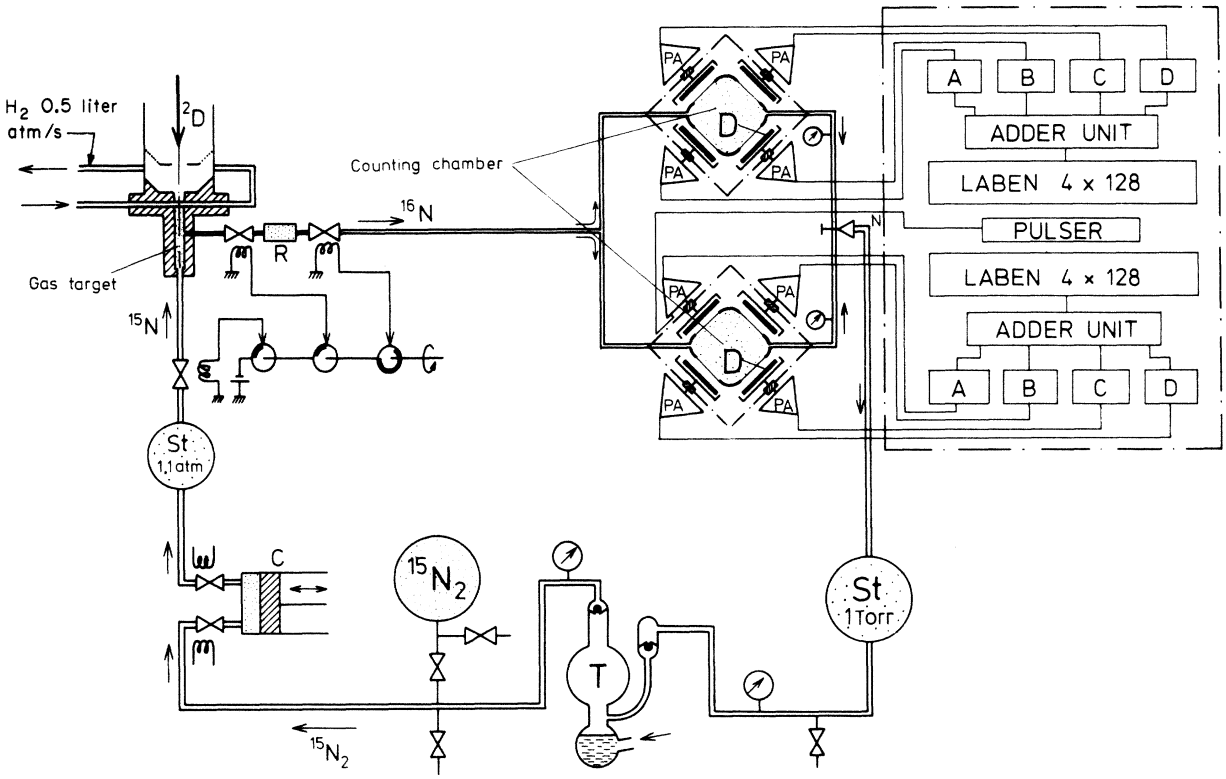

FIG. 2. Schematic view of the experimental layout. D—detector, PA—preamplifier, ABCD—amplifier chains, N—needle valve, St—storage tanks, T—Toepler pump, C—compressor, H_2—hydrogen gas cooling, R—reservoir for ^{16}N.

conserving α particles from the background spectrum. The result of Ref. 9, based on a total of about 10^6 α particles, was stated by the authors as preliminary and is difficult to explain in view of the considerably smaller values obtained in Ref. 10 with about 100 times more α particles.

The present work is a continuation of the investigation presented in the preliminary report (Ref. 10). In these measurements, a technique was applied which combines the production of ^{16}N at high concentrations in gaseous form with an α-particle counting device of high efficiency and good energy resolution.

2. EXPERIMENTAL PROCEDURE

A. General experimental arrangement (see Fig. 2)

Radioactive ^{16}N was produced from the $^{15}N(d,p)$ reaction by bombarding 96% enriched ^{15}N gas at a pressure of 1.1 atm with 3 MeV deuterons from the Max Planck Institute, Mainz, Van de Graaff accelerator. The deuteron beam entered the target cell (a hollow water-cooled cylinder 2 mm in diameter and 30 mm long) through a window of two 5 μm oxydized aluminum foils which were cooled by hydrogen gas flowing between them. The oxidation of the foils inhibited ruptures and resulted in foil lifetimes of about 20 hours for beam currents ≤ 8 μA.

At 5 sec intervals during data acquisition, approximately 10% of the irradiated target gas was transferred into a small reservoir which was connected to two identical counting chambers by a thin nickel capillary tube (1 mm in diameter). A gas pressure of 6–8 Torr was maintained in the counting chambers by continuously exhausting the chambers through a needle valve into a low-pressure (1 Torr) storage tank from which the ^{15}N gas was returned to the target cell by means of a Toepler pump and a small compressor.

Both counting chambers had a spherical volume of 2 cm^3 and were located 1 m from the target cell. Each chamber (see Fig. 3) had four circular windows of 6 mm diameter, each of which was covered by a ~30 μg cm^{-2} collodion foil and viewed by a silicon surface-barrier detector which subtended a mean solid angle of 0.11 ± 0.005 sr. This geometry yielded a counting rate of approximately one α particle per detector per μC of incident deuterons.

Each counting chamber was constructed such

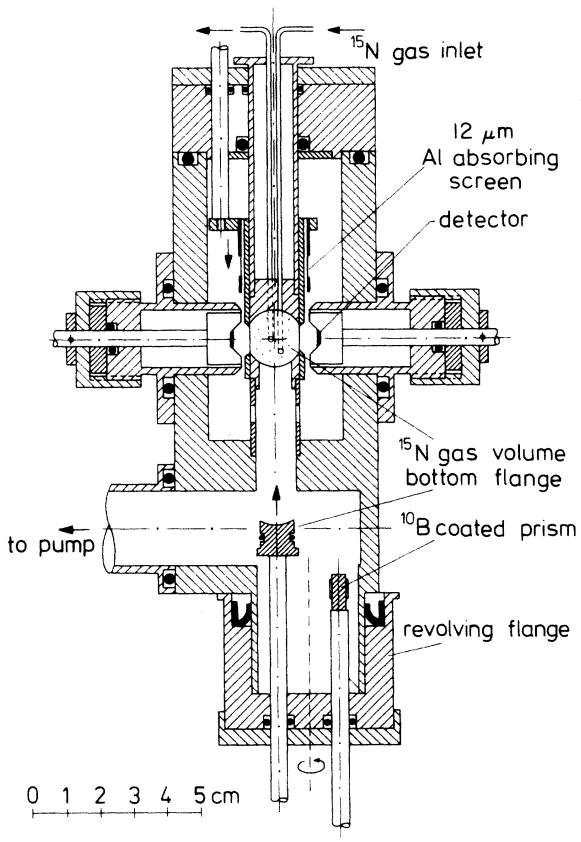

FIG. 3. Counting chamber with detectors and absorbing screens.

that a ^{10}B coated prism could be inserted into the volume normally occupied by the irradiated target gas. It was then possible to determine α-particle energy loss in the collodion foils by using α particles from the $^{10}B(n, \alpha)^7Li^*$, ^{7}Li reaction as discussed in Sec. 2 D below. Only foils with energy losses between 25 and 35 keV for 1.47 MeV incident α particles were used.

B. Detectors

For each α particle from the decay of ^{16}O, approximately 10^5 β particles from the decay of ^{16}N were also expected, resulting in a β-particle contribution to the α-particle spectrum. In order to minimize the energy loss of these electrons in the detector, partially depleted Ortec A-018-025-100 surface-barrier detectors of low-resistivity (435 Ω cm) silicon were used, and the lowest possible operating voltage still giving a good peak response was applied to the detectors. This corresponded to a depletion depth of 35 μm, giving an energy loss of about 30 keV for fast electrons while completely stopping α particles of energies up to 6 MeV.

The α-particle energy loss in the gold surface layer of each detector was measured by using a magnetically analyzed $^4He^{+2}$ beam from a 1.5 MeV accelerator. The angle at which the incident beam impinged on a detector was varied, and the energy loss was determined from the corresponding change in energy of the detected α particles. For 1.5 MeV α particles at normal incidence to the gold layer, the energy loss for individual detectors was found to vary between 10 and 20 keV and was obtained for each detector with an accuracy of ±2.5 keV.

The 1.5 MeV $^4He^{+2}$ beam was also used to determine the α-particle resolution for each detector, both before and after it had been used for data acquisition. This insured that the detector resolution contribution to the α-particle response function of the detecting system (see Sec. 2 E) remained constant. Only detectors with resolutions between 12 and 18 keV were used.

C. Electronics

During data acquisition a counting rate in the detectors of about 5 α particles and 5×10^5 β particles per second was expected. For this reason, the electronics were chosen mainly to minimize the contributions to the α-particle resolution of pulse pileup in the detectors and of electronic noise. Each detector was connected to a separate amplifier chain in which pulses corresponding to an energy $\leq$500 keV were eliminated. Each amplifier-chain output was then routed into a separate 128-channel subgroup of one of two 512-channel Laben multichannel analyzers (MCA's) (see Fig. 2). For 80% of the data, the Laben MCA's were used; however, to determine whether analyzer peculiarities were important, the last 20% of the data was taken with a 4096-channel Hewlett-Packard MCA. The amplifier-chain output for each detector was, in this case, routed into separate 512-channel subgroups, which were later reduced to 128-channel spectra by summing every four adjacent channels. Since the energy interval between channels for 128-channel spectra was kept the same for all three MCA's, all pulse-height distributions could be compared or added channel by channel.

The differential nonlinearity of the Laben MCA's was determined using a sliding pulser and was found to be about 1%. Since the number of counts per channel due to the expected α-particle group from the parity non-conserving decay was estimated to be also about 1% of the main spectrum produced by the allowed α-particle decay of the 9.60 MeV state, this differential nonlinearity had to be reduced by at least an order of magnitude. This was achieved by the following averaging procedure. The MCA's were modified in order to al-

low the arbitrary shifting of the whole pulse-height distribution by applying a variable subtraction step to the incoming pulses. Every two hours during data acquisition, the accumulated pulse-height spectrum was stored, and the MCA's cleared. The subtraction step was then applied such that the new spectrum would be displaced by one channel from the previous one. This procedure was used for each consecutive spectrum until a maximum displacement of 25 channels was reached. The channel shifting was then reversed, and the spectrum stepped back over the 25 channels in the opposite direction. The individual spectra were realigned by the computer before being summed or compared. When the Hewlett-Packard pulse-height spectra were reduced to 128 channels, the differential nonlinearity was less than 0.1%; thus no averaging by spectrum displacement was necessary.

D. Energy calibration of the analyzing system

For the absolute energy calibration of each detector and its respective amplifier chain, 5.48 MeV α particles from ^{241}Am were used to determine a high energy point, and α particles from the reaction of thermal neutrons with ^{10}B were used for the region of the experiment (1–2 MeV). In this latter case, magnetically analyzed 2 MeV protons from the Van de Graaff accelerator bombarded a metallic lithium target producing neutrons from the ^{7}Li(p, n) reaction. The neutrons were thermalized in paraffin and allowed to react with the ^{10}B coated prism (see Sec. 2 A and Fig. 3), which had been inserted into the counting volume, producing α particles from the ^{10}B$(n, \alpha)^{7}$Li*, ^{7}Li reaction ($E_\alpha^* = 1472.3 \pm 0.9$ keV and $E_\alpha = 1776.5 \pm 0.7$ keV for thermal neutrons). Since the layer of ^{10}B on the prism was thick (≈ 1 mg cm^{-2}), the pulse-height spectrum for each α-particle energy is represented by the integral of a Gaussian function. This integral was approximated by a trapezoidal curve (see Fig. 4), the midpoint of which defined the respective energy, E_α^* or E_α, minus the α-particle energy loss in the gold surface layer of the detectors. The maximum error in this approximation, which also included the uncertainty for the α-particle energy loss in the collodion foils, was estimated to be ±3.5 keV. The combination of this error with the uncertainty in the α-particle energies (±1 keV) and the uncertainty for the energy loss in the detector gold layers (±2.5 keV) yielded a maximum estimated error in the absolute calibration of the energy scale of ±4.5 keV in the vicinity of 1.5 MeV.

The relative energy scale for each amplifier chain was determined using a precision pulser which was connected to the individual preamplifier inputs. The amplified pulse height was measured to one part in 10^5 with a digital voltmeter, and when plotted against channel number in the MCA's (see Fig. 4), demonstrated an integral nonlinearity for the energy scale of ±0.7% in the Laben MCA's and of ±0.75% in the Hewlett-Packard MCA.

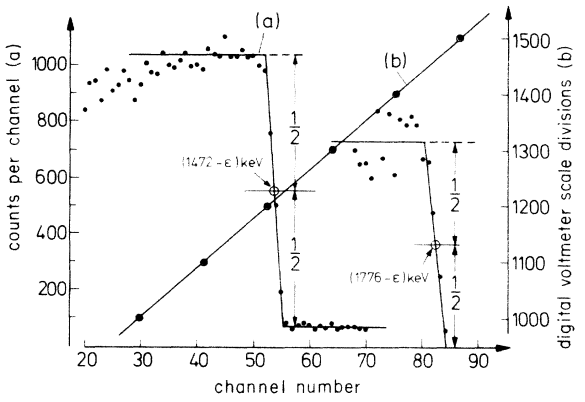

FIG. 4. (a) Pulse-height distribution of the α particles from the ^{10}B$(n, \alpha)^{7}$Li*, ^{7}Li$_{g.s.}$ reaction, giving the calibration points (1472–ϵ) keV and (1776–ϵ) keV, where ϵ is the energy loss in the front layer of the detector; (b) precision pulser pulse height against digital voltmeter scale divisions, indicating the conversion of the digital voltmeter scale into α-particle energies.

E. α-particle response function

The α-particle response function of the detecting system, i.e., the pulse-height distribution produced in the MCA's by a group of monoenergetic α-particles originating in the gas of the counting chamber, depended mainly on three factors: electronic resolution, detector resolution (see Sec. 2 B), and counting chamber geometry.

The resolution of the electronics (including effects of pulse pileup in the detectors) was determined with a precision pulser which was connected to the preamplifier input while α particle counting from the sequential decay of ^{16}N was in progress. The pulse height of the pulser peak was adjusted to correspond to the energy (1.28 MeV) of α particles from the decay of the 8.87 MeV state in ^{16}O. The full width at half maximum (FWHM) of this pulser peak was found to be a linear function of the total counting rate, increasing from 25 keV for zero α-particle intensity to 29 keV for five α particles per second entering the detector. This latter counting rate was adopted as a standard and maintained during all measurements.

The expected energy spectrum for monoenergetic α particles emitted from arbitrary points inside the spherical volume of the counting chamber was calculated by integrating the α-particle energy

loss over the different path lengths in the ^{15}N gas, the collodion foil window, and the detector gold layer. (The small additional contribution to this energy spectrum from the recoil of the ^{16}O nucleus in the β decay of ^{16}N was neglected because it is a function of an unknown amount of mixing of Fermi and Gamow-Teller transitions.) When this energy spectrum is combined with the electronic and detector resolutions, a calculated response function for the detecting system results, which is shown by the solid line in Fig. 5(a) for 1.28 MeV α particles in nitrogen gas at 7 Torr and a particular set of detector characteristics. The broken line in Fig. 5(a) represents a Gaussian function with the same peak height and width (FWHM = 40 keV) as the calculated response function and contains about 95% of the area defined by the response function. The mean energy shift

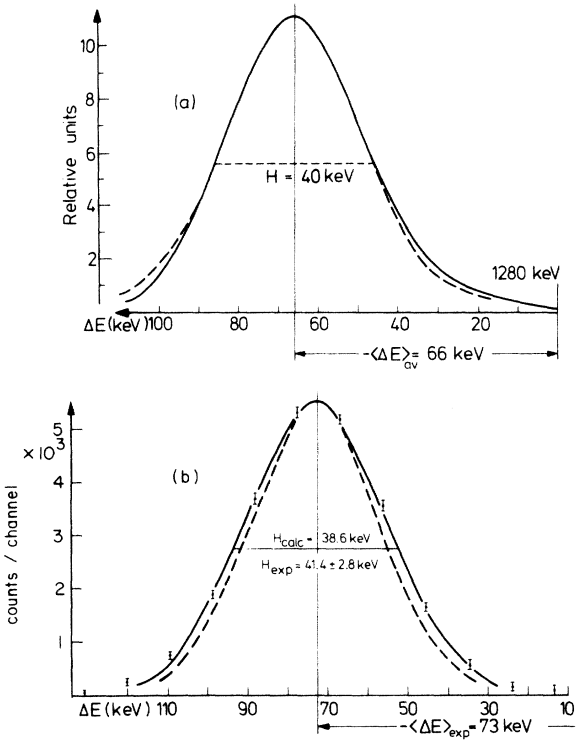

FIG. 5. (a) Calculated response function and energy shift $\langle \Delta E \rangle_{av}$ for monoenergetic α particles with an energy of 1280 keV. The dashed line shows a Gaussian with the same FWHM, H. The calculation was performed for the following parameters: N_2 pressure = 7 Torr, collodion foil window thickness = 30 keV, detector resolution = 18 keV, detector gold layer thickness = 20 keV. (b) Measured response function for 1.47 MeV α particles from the $^{10}B(n, \alpha)$ reaction in trimethylborate vapor. The solid line shows the best Gaussian fit through the points, and the dashed curve shows the calculated response function for this experimental arrangement.

$\langle \Delta E \rangle_{av}$, from α-particle energy loss in the ^{15}N gas, the collodion foil window, and the detector gold layer, was determined for each detector and collodion foil, allowing each individual pulse-height spectrum to be corrected to give true α-particle energies.

To test the calculated response function, one of the counting chambers was filled with trimethylborate vapor $[B(CH_3O)_3]$ at a pressure of 2 Torr, which is equivalent to nitrogen gas at a pressure of 7 Torr with respect to α-particle energy loss. Oxydized aluminum foils, with an energy loss of 42 keV for 1.47 MeV incident α particles normal to the surface, replaced the collodion foils. Thermalized neutrons from the $^7Li(p, n)$ reaction were used to produce α particles from the $^{10}B(n, \alpha)$ reaction as discussed in Sec. 2 D. The measured α-particle pulse-height distribution is presented in Fig. 5(b) where the solid line represents the best Gaussian fit to the experimental data and yields a FWHM of 41.4 ± 2.8 keV. The calculated response function for this experiment is shown by the broken line in Fig. 5(b) and has a FWHM of 38.6 keV. Since the experimental FWHM differs from the calculated value by only 1 standard deviation, the calculated response function reasonably represents the experimental system and, as shown in Sec. 3 B, an uncertainty of $\approx 10\%$ in the width of the response function has only a small influence on the final result of the experiment.

F. Background

The three most probable contributions to background in the α-particle spectrum from the sequential decay of ^{16}N were: (i) particles from neutron induced reactions in the detectors and their surroundings, (ii) β particles from the decay of ^{16}N, and (iii) particles from deuteron induced activity in impurities in the ^{15}N target gas.

Neutrons, primarily from the $^{15}N(d, n)$ reaction in the target cell, produced a background from (n, p) and (n, α) processes in the detectors and their surroundings. This background was measured with the ^{15}N gas flow stopped, so that the α-particle decay of ^{16}O was not detected; however, the neutron flux in the counting chambers was undisturbed. After shielding the target cell with 10 cm of lead and 70 cm of boron-impregnated paraffin, the background from these neutron induced reactions was reduced to less than 10^{-3} of the number of α-particle counts in each channel.

In the energy region below 1.3 MeV, the main contribution to the background was β particles from the decay of ^{16}N. The β-particle spectrum was measured with 12 μm aluminum foil absorbers situated between the collodion foil windows

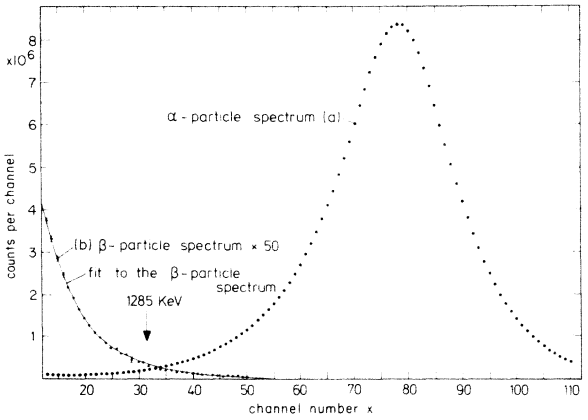

FIG. 6. (a) Pulse-height distribution of 2.5×10^8 α particles. The arrow indicates the position of the expected parity non-conserving α-particle group. The errors are smaller than the size of the points. (b) Pulse-height distribution of the β-particle spectrum on a fifty-fold enlarged scale. The solid line shows the result of a least-squares fit to the points using Eq. (3.1).

and the detectors (see Fig. 3), such that α particles with energies less than 3 MeV were completely stopped in the absorbers while β-particle energy loss was minimal. During data acquisition, β-particle spectra were measured using the aluminum foil absorbers for 7% of the total counting time. The total β-particle spectrum, normalized to the total α-particle counting time, is presented as the set of data points labeled (b) in Fig. 6 and in channel 32 (1.28 MeV) contributes about 3% to the total α-particle spectrum which is shown by the set of data points labeled (a) in Fig. 6.

To determine the background contribution from deuteron induced activity in impurities in the ^{15}N target gas, pulse-height spectra were measured for air and for ordinary nitrogen which were the primary contaminants in the gas system. These spectra corresponded within statistical limits to the natural ^{15}N content of these gases. Thus, any contribution by these contaminants to the normal α-particle counting rate was <0.05% in each channel.

G. Data acquisition

Approximately 2000 hours of beam time were used to obtain the present results. At the end of each two hours the measured pulse-height spectra were recorded on tape, after which the stability of the MCA's and the amplifier chains was checked using two pulser peaks separated in energy by 678 keV (10.59 keV per channel). This energy separation had been chosen such that the pulser counts at each energy would fall equally into a pair of adjacent channels, e.g. channels 33/34 and channels 97/98. A shift in amplifier gain or in MCA zero point or integral linearity could thus be detected with an accuracy of ±0.1 channels. The maximum shift allowed was ±0.5 channels, and the few runs with larger fluctuations were rejected.

The analyzing system was checked daily to exclude the possibility that features seen in the pulse-height spectra could have been produced by instrumental anomalies. This was accomplished by the following test procedure. Four ^{241}Am sources had been mounted on the faces of a small rectangular prism and covered by appropriate absorbing foils in order to give broad smooth α-particle spectra resembling those from the sequential decay of ^{16}N. The prism was inserted into each counting chamber in turn, and pulse-height spectra measured under the same conditions as for those pulse-height spectra from the decay of ^{16}O, including averaging by spectrum displacement. The intensity of these ^{241}Am sources was chosen to allow α-particle counting rates about 100 times higher than those with ^{16}N. The analysis of these spectra is presented in Sec. 3 A.

At the end of each 50 hours, α-particle data acquisition was stopped, and β-particle spectra were measured (see Sec. 2 F). α particles from the ^{10}B(n, α) reaction were then used to check the energy calibration of the analyzing system (see Sec. 2 D) and collodion foil window thicknesses (see Sec. 2 A).

H. Relative ^{16}N β branching ratios to the 9.60 MeV (1^-) and 8.87 MeV (2^-) states in ^{16}O

To calculate the α-particle emission width Γ_α of the 8.87 MeV state in ^{16}O, the relative ^{16}N β branching ratio to the 9.60 MeV state and the 8.87 MeV state is required (see Sec. 3 B). This branching ratio is defined by

$$R = \frac{N_\beta(9.60)}{N_\beta(8.87)}, \tag{2.1}$$

where $N_\beta(9.60)$ and $N_\beta(8.87)$ are the number of β particles from the decay of ^{16}N which leave the daughter ^{16}O nuclei in the 9.60 MeV and 8.87 MeV states, respectively. Since essentially all of the 9.60 MeV state decays by α-particle emission, $N_\beta(9.60)$ is well approximated by the number of α particles from this decay, $N_\alpha(9.60)$. The 8.87 MeV state decays by γ-quantum emission to the 6.13 MeV state with $76\pm3\%$ probability[11] allowing the indirect measurement of $N_\beta(8.87)$ by counting these γ quanta: $N_\beta(8.87) = [N_\gamma(8.87)]/0.76$, where $N_\gamma(8.87)$ is the number of γ quanta from the 8.87 → 6.13 MeV transition. If the 1.77 MeV α particles from the decay of the 9.60 MeV state in ^{16}O are then measured simultaneously with the 2.74 MeV

γ quanta from the decay of the 8.87 MeV state in ^{16}O, and if the efficiencies (ϵ_α and ϵ_γ) and subtended solid angles (Ω_α and Ω_γ) of the detectors are known, R in Eq. (2.1) can be determined from

$$R \cong \frac{0.76 N'_\alpha(9.60)\epsilon_\gamma \Omega_\gamma}{N'_\gamma(8.87)\epsilon_\alpha \Omega_\alpha}, \tag{2.2}$$

where $N'_\alpha(9.60)$ and $N'_\gamma(8.87)$ are the 1.77 MeV α-particle and 2.74 MeV γ-quantum counts from the respective detectors.

For this measurement, a counting chamber with a cylindrical gas volume and one ~30 $\mu g\,cm^{-2}$ collodion foil window was used. The collodion foil window was viewed by a detector of the same type and in the same geometry as described in Secs. 2 A and 2 B. It was directly opposed by a 50 cm^3 coaxial Ge(Li) detector situated on the other side of the counting chamber. The factor $\epsilon_\gamma \Omega_\gamma$ in Eq. (2.2) was determined for the Ge(Li) detector in this geometry by measuring the ratio of the number of β particles from a ^{24}Na source in coincidence with the γ quanta from the 4.12 → 1.37 MeV transition in the daughter ^{24}Mg nuclei to the total number of β particles from the ^{24}Na source.

The relative ^{16}N β branching ratio R was then measured with ^{15}N gas in the detection system, as described in Sec. 2 A above, and was found from Eq. (2.2) to be $(9.98 \pm 0.70) \times 10^{-4}$. This value for R is some 11% smaller than that used in the preliminary report (Ref. 10).

3. DATA ANALYSIS

The total ^{16}O α-particle pulse-height spectrum from all measurements is shown by the data points labeled (a) in Fig. 6. In this spectrum the β-particle contribution (see Sec. 2 F) has not been subtracted; the measured β-particle spectrum is shown by the data points labeled (b) (on a fifty-fold enlarged scale). Channel 32 (designated by an arrow) corresponds to an α-particle energy of 1285 keV which would be expected for α particles from the decay of the 8.87 MeV state in ^{16}O.

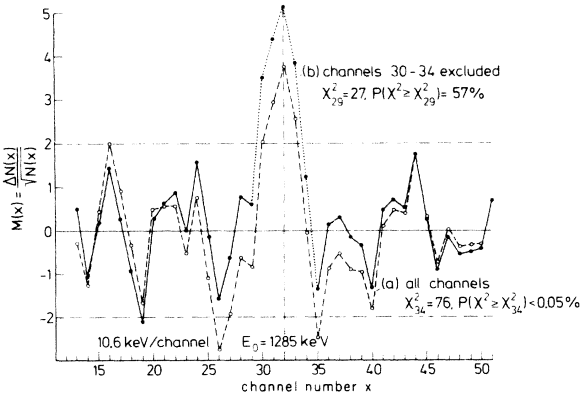

FIG. 7. Deviations $M(x)$ of the measured pulse-height distribution [Fig. 6(a)] from the least-squares fit with Eq. (3.1): (a) all the channels, 13–51, included for the fit; (b) fit with channels 30–34 omitted.

A. Statistical analysis of the α-particle spectrum around 1285 keV

For the 39 channels (13–51) which correspond to an energy interval of 413 keV the α-particle spectrum was fitted, using the method of least squares, by the smooth function

$$W(x) = A \exp(-\alpha x) + B \exp(\beta x) + C, \tag{3.1}$$

where $W(x)$ is the number of events in channel x and A, α, B, β, and C are the parameters to be determined. The least-squares fit yielded a χ^2_{34} (where f, the number of degrees of freedom, is 34) equal to 76, which corresponds to a probability $P(\chi^2 \geq \chi^2_{34}) < 0.05\%$. The largest contribution to χ^2 comes from the five adjacent channels, 30–34. This can be seen in curve (a) in Fig. 7 in which the ordinate function $M(x)$ is the deviation of the measured pulse-height distribution for each channel x from the least-squares fitted curve, defined in units of the standard deviation

$$M(x) = [\Delta N(x)] / [N(x)]^{1/2}, \tag{3.2}$$

where $N(x)$ is the number of events recorded in channel x and $\Delta N(x) = N(x) - W(x)$. A second least-squares fit of Eq. (3.1) was made for the interval $x = 13$–51 omitting channels 30–34 and yielded a χ^2_{29} of 27 with a corresponding probability $P(\chi^2 \geq \chi^2_{29}) = 57\%$. The deviations $M(x)$ for this fit are plotted as curve (b) in Fig. 7.

If the number of events in channels 30–34 is summed and statistically treated as one channel (X_{30-34}), the total deviation $[M_{30-34}]$ of X_{30-34} from the least-squares fitted curve can be defined in units of the standard deviation as

$$[M_{30-34}] = \frac{1}{\sqrt{5}} \sum_{x=30}^{34} M(x). \tag{3.3}$$

For the least-squares fit of Eq. (3.1) to the measured α-particle spectrum $[M_{30-34}] > 5$; i.e., it is farther than 5 standard deviations from the fitted curve. Since the direction (positive or negative) of the individual deviations $M(x)$ is preserved by Eq. (3.2), the positive value of $[M_{30-34}]$ corresponds to a positive excess in the measured pulse-height data which, in this case, is statistically significant.

This statistically significant positive excess in the interval $x = 30$–34 could be a measured α-particle energy distribution, or it could be caused by (i) the β-particle contribution to the α-particle

TABLE II. Results of the least-squares fits to Eq. (3.1) for the eight detectors.

Detector (j)	All channels $[M_{30-34}(j)]$	χ^2_{34}	Channels 30–34 excluded $[M_{30-34}(j)]$	χ^2_{29}
1	2.01	39	3.18	28
2	1.05	58	1.84	46
3	2.41	50	3.49	38
4	2.07	31	3.36	21
5	1.80	26	3.12	17
6	1.76	34	2.48	18
7	0.96	33	1.39	31
8	1.92	38	3.46	28

$$[M_{30-34}] \cong \frac{1}{\sqrt{8}} \sum_{j=1}^{8} [M_{30-34}(j)]$$

$$= 13.98/\sqrt{8} = 4.94 \qquad = 22.32/\sqrt{8} = 7.89$$

spectrum, (ii) peculiarities in an amplifier chain or detector, and/or (iii) MCA pecularities including differential nonlinearity. These possibilities are discussed in the following paragraphs.

(i) The measured β-particle spectra, when least-squares fitted by Eq. (3.1) in the interval $x = 13$–51, yielded a $[M_{30-34}] < 1$; the fitted curve is plotted in Fig. 6. However, to explain the positive excess in the α-particle spectrum as structure from the β-particle contribution would require an $[M_{30-34}] > 8$ for this β spectrum.

(ii) The α-particle pulse-height spectra from all eight amplifier chains with their respective detectors were individually least-squares fitted to Eq. (3.1) both including and excluding channels 30–34. The results of these fits are given in Table II. The χ^2's for both sets of fits fall within $f \pm 2\sqrt{2f}$ (except for detector 2), indicating the statistics for any given detector j are insufficient to determine a positive excess in channels 30–34. However, $[M_{30-34}(j)]$ for each detector has a positive sign and increases in value when channels 30–34 are excluded from the least-squares fit. The large χ^2 ($\chi^2 > f + 2\sqrt{2f}$) for detector 2 cannot be attributed to a deviation in the channels 30–34 since $[M_{30-34}(2)]$ is only 1 standard deviation. The sum of the $[M_{30-34}(j)]$'s for the individual detectors agrees well with the total deviation $[M_{30-34}]$ as can be seen from a comparison of Tables II and III. A peculiarity in one amplifier chain or detector, thus, does not account for the positive excess in channels 30–34.

(iii) Since the ^{241}Am spectra discussed in Sec. 2 G were measured under the same conditions as the α-particle spectrum from ^{16}O, they were used to investigate MCA peculiarities and differential nonlinearity. The total ^{241}Am spectrum contained $>10^6$ events per channel and is plotted in Fig. 8 for the energy domain relevant to the experiment. The small standard deviation per channel $\{[N(x)]^{1/2}/N(x) < 0.1\%\}$ for this spectrum allowed a sensitive evaluation of differential nonlinearity in the MCA's; Eq. (3.1) was used for the least-squares fit and the individual $M(x)$'s are plotted against channel number in Fig. 9(a) for the interval $x = 18$–54. The resultant $\chi^2_{31} = 120$ indicates these deviations are not of statistical origin but rather demonstrate MCA nonlinearity. When the deviations are replotted as percentages in Fig. 9(b), it can be seen that the average differential nonlinearity is less than 0.1% and in the interval $x = 30$–34 is more in the neighborhood of 0.03%. Since the positive pulse-height excess from ^{16}O is almost 1% of the total number of events in channels 30–34, the MCA differential nonlinearity or peculiarity as seen in the ^{241}Am spectrum cannot account for this excess.

As a further check on MCA peculiarity, the Hewlett-Packard data alone were analyzed; these results together with the results for all the data are presented in Table III. The ratio of the deviation $[M_{30-34}]$ for all the data to the deviation $[M_{30-34}]$

TABLE III. Deviations of the five adjacent channels 30–34.

	$[M_{30-34}]$ Fit with all the channels (13–51)	Fit with channels 30–34 omitted
All data (2.5×10^8 α particles)	5.1	8.2
Hewlett Packard data (5.4×10^7 α particles)	2.56	3.8
$\frac{[M_{30-34}](\text{All data})}{[M_{30-34}](\text{H-P data})} \times \left[\frac{5.4}{25}\right]^{1/2}$	0.92 ± 0.44	1.00 ± 0.47

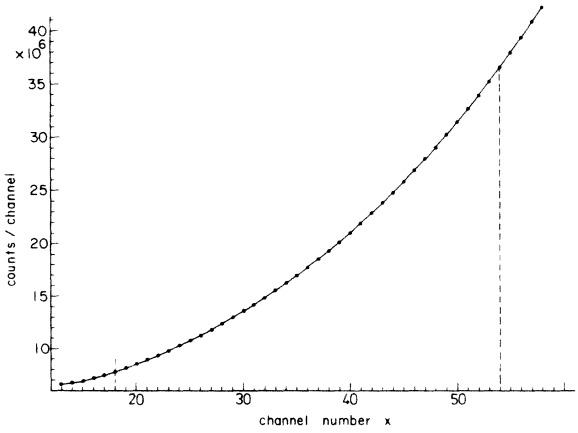

FIG. 8. Pulse-height distribution from the ^{241}Am test runs. The curve represents a least-squares fit to the points with Eq. (3.1).

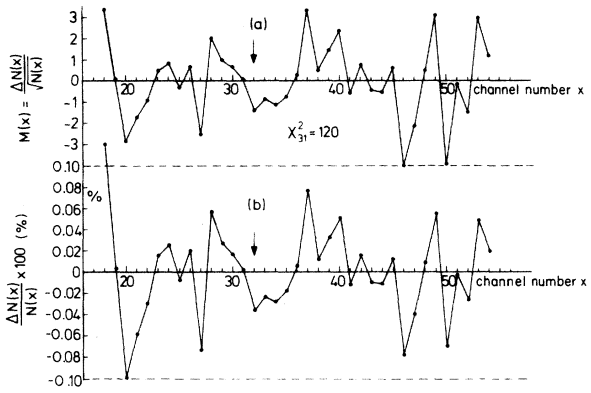

FIG. 9. Deviations of the measured points from the least-squares fit as given by Fig. 8 (a) in units of the standard deviation and (b) in percent.

for the Hewlett-Packard data, adjusted for counting statistics, should be equal to 1 if both sets of data show the same percentage deviation in the interval $x = 30$–34. The poor statistics for the Hewlett-Packard data give rise to a large uncertainty in the value of this ratio in Table III, but since within this uncertainty the ratio is 1 and since $[M_{30-34}]$ for the Hewlett-Packard data is positive, MCA peculiarity cannot account for the positive pulse-height excess.

The foregoing investigations indicate that the positive excess for channels 30–34 in the measured pulse-height distribution (Fig. 6) is an energy distribution of α particles corresponding from kinematics to the decay of the 8.87 MeV state in ^{16}O.

B. α particles from the decay of the 8.87 MeV state in ^{16}O

Assuming the energy distribution of the α particles responsible for the positive pulse-height excess belongs to a monoenergetic group, a Gaussian function was chosen for the form of this distribution according to the results obtained in Sec. 2 E. To determine the energy of this group, a function $W'(x)$ was constructed by adding a Gaussian to the function $W(x)$ given by Eq. (3.1):

$$W'(x) = W(x) + D \exp[-(x_0 - x)^2 4(\ln 2)/H^2], \quad (3.4)$$

where D is the number of events in channel x_0, the axis of symmetry of the Gaussian, and H is the FWHM. The α-particle pulse-height spectrum in Fig. 6 was least-squares fitted by Eq. (3.4) in which A, α, B, β, C, and D were determined by the fit. The value of H was taken from the calculated response function (see Sec. 2 E), and x_0 was sequentially allowed to take on the value of each channel number from 16 to 48. The χ^2_{31} for each

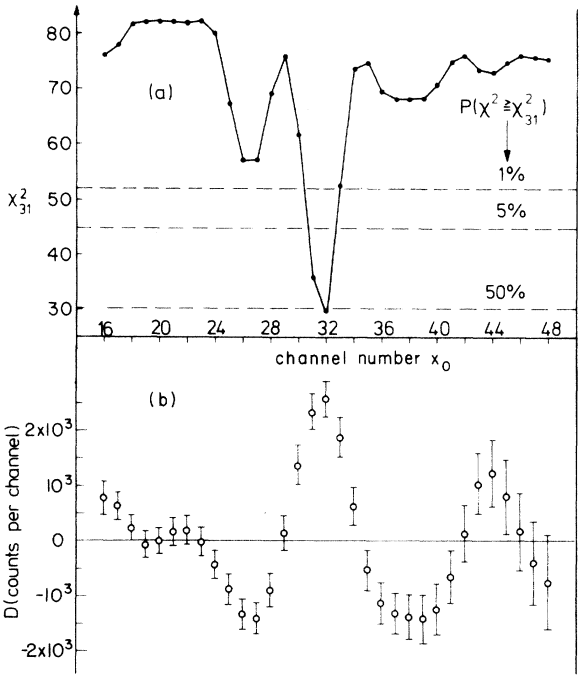

FIG. 10. (a) The values for χ^2 from the least-squares fit to the experimental points in Fig. 6(a) with Eq. (3.4) as a function of the position of the axis of symmetry of the Gaussian, x_0. (b) Number of events D in channel x_0 as determined by the fit in (a).

x_0 is plotted against x_0 in Fig. 10(a); the corresponding value of D is plotted against x_0 in Fig. 10(b). On the basis of the χ^2 minimum in Fig. 10(a), x_0 was restricted to the domain $31 \leq x_0 \leq 33$ and, along with H, determined by the least-squares fit. With a minimum χ^2 $[\chi^2_{31}(\min)]$ of 27.97, x_0 was found to be 31.7 with a corresponding H of 36.2 keV. In view of the calculations given in Sec. 2 E, this value of H is somewhat less than one would expect for the mean from the different detectors used during the measurements, but still within the error of 10% determined for this quantity; in Table IV the variation of $\chi^2_{31}(\min)$

TABLE IV. Values for χ^2_{31} (min), D, and N'_α (8.87) from a least squares fit with $x_0 = 31.7$ as a function of the FWHM H of the Gaussian.

H (keV)	χ^2_{31} (min)	D	N'_α (8.87)
42.4	28.94	2532	10770
39.1	28.19	2581	10100
37.0	27.99	2611	9713
36.2	27.97	2623	9538
35.3	28.00	2635	9350
33.3	28.14	2650	9050
31.2	28.65	2680	8549

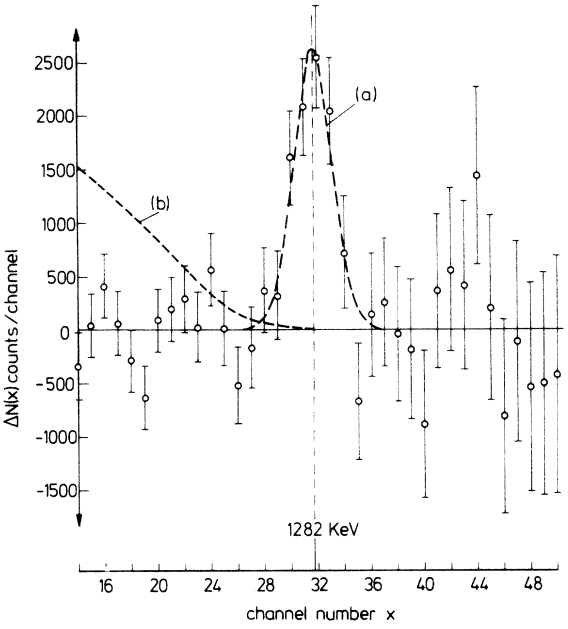

FIG. 11. The points represent the deviations of the experimental values given by Fig. 6(a) from the function $W(x)$ in Eq. (3.4). Curve (a) is the best fit Gaussian with $D = 2623$ and $H = 36.2$ keV. Curve (b) represents the α-particle distribution given by Eq. (4.2) in arbitrary units.

and D with different values of H is shown. In Fig. 11 the deviations of the measured values from $W(x)$ in Eq. (3.4), $\Delta N(x)$, are plotted against channel number, and the Gaussian part of Eq. (3.4) $[W'(x) - W(x)]$ is plotted as curve (a) for $x_0 = 31.7$ and $H = 36.2$ keV. This value for x_0 corresponds to an energy $E_0 = 1282$ keV with a maximum estimated error from Sec. 2 D of ±4.5 keV. Using the level scheme in Fig. 1, the value for E_0 agrees within 1 keV with that calculated for α particles from the decay of the 8.87 MeV state in ^{16}O.

To determine $N'_\alpha(8.87)$, the number of α particles populating the measured peak at 1282 keV, the Gaussian part of Eq. (3.4) was integrated:

$$N'_\alpha(8.87) = \tfrac{1}{2}DH(\pi/\ln 2)^{1/2}. \tag{3.5}$$

For $H = 36.2$ keV, $N'_\alpha(8.87) = 9538 \pm 1810$ detected α particles; the variation of $N'_\alpha(8.87)$ with H is also shown in Table IV. The error calculation for $N'_\alpha(8.87)$ is presented in the Appendix.

To show that the foregoing results are not solely dependent upon the choice of the smooth function Eq. (3.1), two other types of functions with superimposed Gaussians have been used to fit the data of Fig. 6: (i) polynomials of order $p = 3-7$ and (ii) a Breit-Wigner distribution.[12] The results for all three types of functions are presented in Table V; only the polynomial $p = 5$ is quoted since it was sufficient to give a $P(\chi^2 \geq \chi^2_f)$ close to 50%.

Since the levels in ^{16}O are populated entirely by the β-particle decay of ^{16}N, the α-particle emission width Γ_α for the 8.7 MeV state in ^{16}O can be calculated from

$$\Gamma_\alpha = \Gamma \frac{N_\alpha(8.87)}{N_\beta(8.87)}, \tag{3.6}$$

where Γ is the total width of the 8.87 MeV state and $N_\alpha(8.87)$ is the number of α particles which are emitted from $N_\beta(8.87)$ ^{16}O atoms in which the 8.87 MeV state is populated (see Sec. 2 H). Multiplying Eq. (3.6) by the ratio $N_\beta(9.60)/N_\alpha(9.60) \cong 1$ yields

$$\Gamma_\alpha = \Gamma \frac{N_\beta(9.60)}{N_\beta(8.87)} \times \frac{N_\alpha(8.87)}{N_\alpha(9.60)}. \tag{3.7}$$

In this case $\Gamma \cong \Gamma_\gamma$, the total radiation width of the 8.87 MeV state and $N_\beta(9.60)/N_\beta(8.87)$ is the β branching ratio R measured in Sec. 2 H, thus

$$\Gamma_\alpha = \Gamma_\gamma R[N'_\alpha(8.87)/N'_\alpha(9.60)], \tag{3.8}$$

where detector efficiencies and subtended solid angles have been omitted because both α particles are being analyzed in the same detector. Using $\Gamma_\gamma = (2.7 \pm 0.5) \times 10^{-3}$ eV,[13] $N'_\alpha(8.87) = 9538 \pm 1810$, and $N'_\alpha(9.60) = 2.49 \times 10^8$, Γ_α was calculated from Eq. (3.8) to be $(1.03 \pm 0.28) \times 10^{-10}$ eV.

4. DISCUSSION

The group of α particles observed in the present experiment has been identified by its energy as the decay product of the 8.87 MeV state in ^{16}O. A decay of this state into ^{12}C + α may proceed either (i) by a direct parity non-conserving process or (ii) by a multiple parity conserving decay. The simplest parity conserving multiple process is the emission of a γ quantum together with the α particle. Such an electromagnetic transition

TABLE V. Results of fitting three different types of functions by the method of least squares to the measured α-particle pulse-height distribution in Fig. 6.

Type of function	$P(\chi^2 \geq \chi^2(\min))$	x_0 (keV)	H (keV)	D	N'_α (8.87)	$\pm\Delta N'_\alpha$ (8.87)
Exponential [Eq. (3.4)]	52%	1282	36.2	2623	9538	1810
Polynomial ($P = 5$)	40%	1282	35.8	2442	8860	1820
Breit-Wigner	49%	1281	37.8	2611	9925	1980

may proceed from the 8.87 MeV 2^- state to the low energy tail of the 9.60 MeV 1^- state which in turn decays into $^{12}C + \alpha$. Moreover, an electromagnetic transition into the continuum of ^{16}O with subsequent decay into $^{12}C + \alpha$ would in principle be possible. The lowest order electromagnetic transition is in both cases magnetic dipole and leads to an α-particle spectrum of approximately the form

$$f(x) = \text{const}(x_0 - x)^3 P^l(x); x_0 = 31.7, \quad x < x_0, \quad (4.1)$$

where the channel number x stands for the energy of the emitted α particle, $(x_0 - x)$ for the energy of the emitted γ quantum, and $P^l(x)$ for the barrier penetrability of an α particle having an energy corresponding to the channel number x. A decay of this type would give rise to a broad peak with maximum around an energy of 1 MeV, as shown by curve (b) in Fig. 11. The experimental pulse-height distribution shown in Fig. 11 can therefore not be reproduced by such a decay spectrum.

Whether the experimental pulse-height distribution contains both kinds of transitions, i.e., a direct parity non-conserving decay into $^{12}C + \alpha$ as well as the foregoing described multiple decay, has also been investigated. Equation (3.4) was extended by adding Eq. (4.1);

$$W''(x) = W'(x) + G(x_0 - x)^3 P^l(x), \quad (4.2)$$

and the pulse-height distribution in Fig. 6 then fitted by Eq. (4.2) in which the parameters A, α, B, β, C, D, and G were determined by the fit. The parameter G obtained in this way turned out to become negligibly small ($G \approx -4$), while all the other parameters remained essentially the same as obtained by fitting Eq. (3.4). This result excludes a substantial contribution from the proposed multiple process to the decay of the 8.87 MeV state.

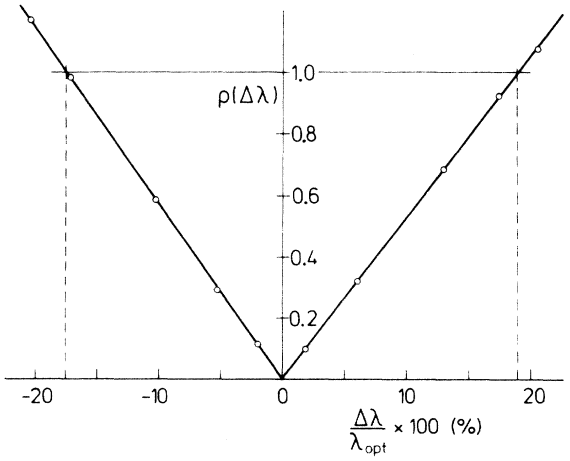

FIG. 12. $\rho(\Delta\lambda)$ as a function of the variation of λ, $\Delta\lambda$.

It is possible to postulate other multiple, parity conserving processes which involve the emission of soft photons or low energy electrons accompanying the α-particle decay, e.g., internal bremsstrahlung or orbital electron emission. While it is very difficult quantitatively to assess the contributions that might come from such sources it seems most unlikely that processes of this type could be strong enough to produce the observed effect.

It is from these considerations that the authors propose to attribute the group of α particles observed in the present experiment to the parity non-conserving decay from the $^{16}O(8.87\ \text{MeV}\ 2^-)$ state into $^{12}C + \alpha$.

The numerical value for the width Γ_α, as determined from the experiment, is in good agreement with recent theoretical calculations[14-18] done by the use of the conventional model of weak interactions. It should be noted, however, that notwithstanding the conformity between the experiment and the conclusions drawn from this model, the experimental result does not contradict the existence of extra currents, as these show very little effect in weak $\Delta T = 0$ interactions.

For a detailed discussion on these theoretical investigations, we would like to refer to a recent review article.[18]

ACKNOWLEDGMENTS

We are greatly indebted to Dr. Mason for his invaluable help in writing the manuscript. We thank Professor Ziegler and Dr. Gari for illuminating discussions. Dr. Jochim's helpful proposal to anodyze the target foils is gratefully acknowledged. We thank Dr. Miller and Dr. Hughes for reading the manuscript and Mr. Kudszus for performing the numerical calculations.

APPENDIX

The number of α particles, $N'_\alpha(8.87)$, is given by Eq. (3.5) as the area under the Gaussian part of Eq. (3.4). By taking this quantity as a parameter λ $[\lambda_{\text{opt}} \equiv N'_\alpha(8.87) = 9538]$, it can be introduced in Eq. (3.4):

$$W'(x, \lambda) = W(x) + D\exp[-\pi D^2(x_0 - x)^2/\lambda^2]. \quad (A1)$$

The standard deviation of λ, $\sigma(\lambda)$, can now be determined with the help of the formula[19]

$$\rho(\Delta\lambda) = [\chi^2(\lambda_{\text{opt}} + \Delta\lambda) - \chi^2(\lambda_{\text{opt}})] \times \left[\sum_{x=13}^{51} [W'(x, \lambda_{\text{opt}} + \Delta\lambda) - W'(x, \lambda_{\text{opt}})]^2/N(x)\right]^{-1/2} = \frac{\Delta\lambda}{\sigma(\lambda)}, \quad (A2)$$

where $\chi^2(\lambda_{opt})$ is the minimum value of χ^2 and $\Delta\lambda$ is the change in λ. When $\rho(\Delta\lambda) = 1$, $\Delta\lambda$ represents the error in the parameter λ, $\sigma(\lambda)$. $\rho(\Delta\lambda)$ has been calculated as a function of $\Delta\lambda$ with the help of least-squares fits and is illustrated by Fig. 12, from which $\sigma(\lambda)$, e.g. the error of $N'_\alpha(8.87)$, has been inferred.

It might be noted that in the case of linear parameters, Eq. (A2) reduces to the well-known formula

$$\chi^2(\lambda_{opt} + \sigma(\lambda)) = \chi^2(\lambda_{opt}) + 1$$

$$= \chi^2_{min} + 1 . \qquad \text{(A3)}$$

---

*Now at Alexander Wiegand, D-8763 Klingenberg/Main, Germany.

[1]D. H. Wilkinson, Phys. Rev. 109, 1603 (1958).
[2]E. M. Henley, Annu. Rev. Nucl. Sci. 19, 367 (1969).
[3]R. E. Segel, J. W. Olness, and E. L. Sprenkel, Phil. Mag. 6, 163 (1961).
[4]D. E. Alburger, R. E. Pixley, D. H. Wilkinson, and P. F. Donovan, Phil. Mag. 6, 171 (1961).
[5]W. Kaufmann and H. Wäffler, Nucl. Phys. 24, 62 (1961).
[6]R. E. Segel, J. W. Olness, and E. L. Sprenkel, Phys. Rev. 123, 1382 (1961).
[7]P. F. Donovan, D. E. Alburger, and D. H. Wilkinson, in *Proceedings of the Rutherford Jubilee International Conference, Manchester, 1961,* edited by J. B. Birks (Academic, New York, 1961), p. 827.
[8]D. P. Boyd, P. F. Donovan, B. Marsh, D. E. Alburger, D. H. Wilkinson, P. Assimakopoulos, and E. Beardsavorth, Bull. Am. Phys. Soc. 13, 1424 (1968).
[9]E. L. Sprenkel-Segel, R. E. Segel, and R. H. Siemssen, in *Proceedings of the Third International Conference on High Energy Physics and Nuclear Structure, Columbia University, New York, 1969,* edited by S. Devons (Plenum, New York, 1970), p. 763.
[10]H. Hättig, K. Hünchen, and H. Wäffler, Phys. Rev. Lett. 25, 941 (1970).
[11]D. H. Wilkinson and D. E. Alburger, Phys. Rev. 173, 995 (1968).
[12]J. Dietz, Ph.D. thesis, Max-Planck-Institute, Mainz, 1972 (unpublished).
[13]M. C. Bertin and R. E. Prixley, Nucl. Phys. A150, 247 (1970).
[14]M. Gari, Phys. Lett. 31B, 627 (1970).
[15]M. Gari and H. Kümmel, Phys. Rev. Lett. 23, 26 (1969).
[16]M. Gari, J. O. Zabelitzky, and H. Kümmel, Nucl. Phys. A161, 625 (1971).
[17]E. M. Henley, T. E. Leliher, and D. U. L. Yu, Phys. Rev. Lett. 23, 941 (1969).
[18]M. Gari, Phys. Rep. 6C, February 1973.
[19]H. Arenhövel, Max-Planck-Institute Report No. 1, 1973 (unpublished).